ACS OMEGA

http://pubs.acs.org/journal/acsodf

Article

Designing Potent α-Glucosidase Inhibitors: A Synthesis and QSAR Modeling Approach for Biscoumarin Derivatives

Thi-Hong-Truc Phan, Kowit Hengphasatporn, Yasuteru Shigeta, Wanting Xie, Phornphimon Maitarad, Thanyada Rungrotmongkol, and Warinthorn Chavasiri*

Cite This: *ACS Omega* 2023, 8, 26340−26350

Read Online

ACCESS | Metrics & More | Article Recommendations | Supporting Information

ABSTRACT: Nineteen biscoumarins were synthesized, well-characterized, and evaluated against α-glucosidases *in vitro*. Of these, six compounds (**10**, **12**, **16**, and **17**−**19**) were newly synthesized and not previously reported in the chemical literature. The majority of the synthesized derivatives demonstrated significant inhibitory activity. A quantitative structure−activity relationship (QSAR) model was developed, revealing a strong correlation between the anti-α-glucosidase activity and selected molecular descriptors. Based on this model, two new compounds (**18** and **19**) were designed, which exhibited the strongest inhibition with IC_{50} values of 0.62 and 1.21 μM, respectively, when compared to the positive control (acarbose) with an IC_{50} value of 93.63 μM. Enzyme kinetic studies of compounds **18** and **19** revealed their competitive inhibition with K_i values of 3.93 and 1.80 μM, respectively. Computational studies demonstrated that compound **18** could be inserted into the original binding site (OBS) of α-glucosidase MAL12 and form multiple hydrophobic interactions with nearby amino acids, with the bromo group playing an essential role in enhancing the binding strength and stability at the OBS of the enzyme based on the quantum mechanical calculations using the fragment molecular orbital method. These findings provide valuable insights into the design of potent α-glucosidase inhibitors, which may have potential therapeutic applications in the treatment of diabetes and related diseases.

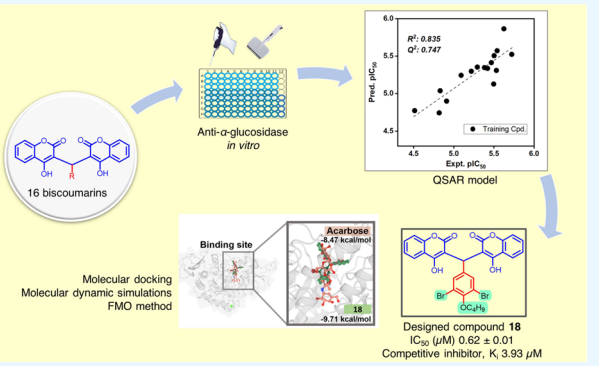

INTRODUCTION

Diabetes mellitus is one of the most common metabolic diseases in the world.[1] The imbalance of glucose homeostasis from diabetes mellitus causes an increase in glucose levels in the blood or hyperglycemia.[2] Type 1 diabetes is due to insulin deficiency, accounting for only 5−10% of the diabetic population, while type 2 diabetes, referred to as noninsulin-dependent diabetes, accounts for 90−95% of cases of diabetes.[1] Diabetes mellitus can lead to serious complications in many parts of the body, such as stroke, blindness, heart attack, kidney failure, and amputation.[3] Alarmingly, the worldwide prevalence of diabetes has been increasing sharply.[2]

α-Glucosidase plays a key role in the digestion of polysaccharides, oligosaccharides, and disaccharides to monosaccharides.[4] α-Glucosidase inhibitors are oral antidiabetic drugs used to treat type 2 diabetes currently[2] since they delay the absorption of sugars from the gut[5] reducing the glucose uptake.[6] Acarbose, miglitol, and voglibose are used as α-glucosidase inhibitors in the market.[1] Acarbose is one of the most widely prescribed α-glucosidase inhibitors in diabetes.[5] Nevertheless, using these α-glucosidase inhibitors might increase the risk of hepatotoxicity[7] and cause gastrointestinal side effects such as flatulence and diarrhea,[8] which is considered a limiting factor for treating diabetes. To discover better safety and efficacy of α-glucosidase inhibitors for drug development, scientists have been continuously further studying diverse compounds including the coumarin scaffold.

Coumarin compounds are oxygen-containing heterocycles with a typical benzopyrone framework that are essential in natural products and organic synthesis. Numerous studies have been proven about multiple potential activities of coumarins, including antiproliferative,[9] anticancer,[10,11] antihepatitis C virus (HCV),[12] antihuman immunodeficiency virus (HIV),[13] anti-Alzheimer,[14] antimalarial,[15,16] antibacterial,[17] antifungal,[18] antioxidant,[19] anticonvulsant,[20] anti-inflammatory,[21] and enzyme inhibition.[22] Coumarins were reported to inhibit several enzymes, *i.e.*, cholinesterase, monoamine oxidase (A and B), aldehyde/aldose reductase, alkaline phosphatase, urease, carbonic anhydrase, lysine-specific demethylase, histone deacetylase, lipoxygenase, topoisomerase, tyrosinase, cyclooxygenase, and α-glucosidase.[22] Many coumarins were

Received: April 26, 2023
Accepted: June 22, 2023
Published: July 11, 2023

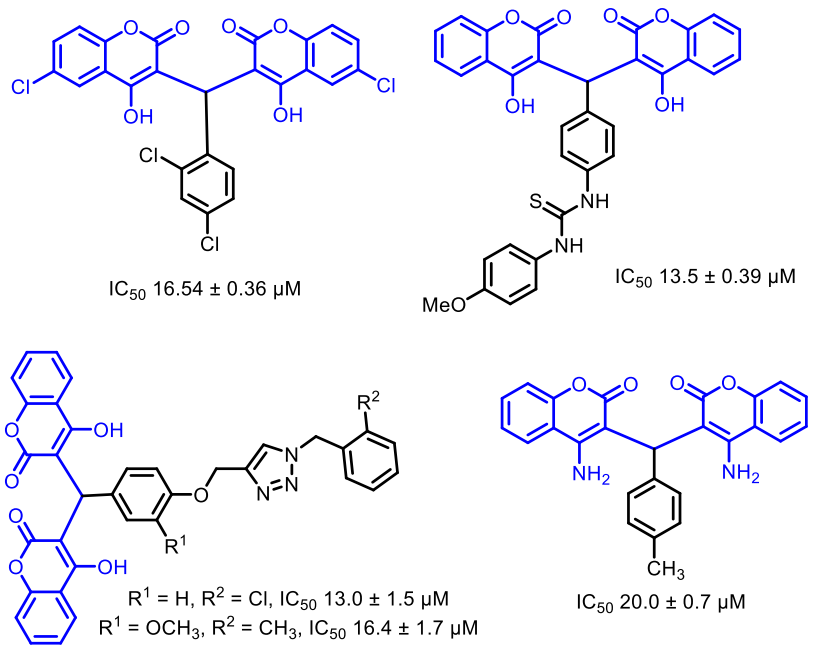

Figure 1. α-Glucosidase inhibitors containing a biscoumarin skeleton.

Scheme 1. Synthesis of Biscoumarin Derivatives 1−16

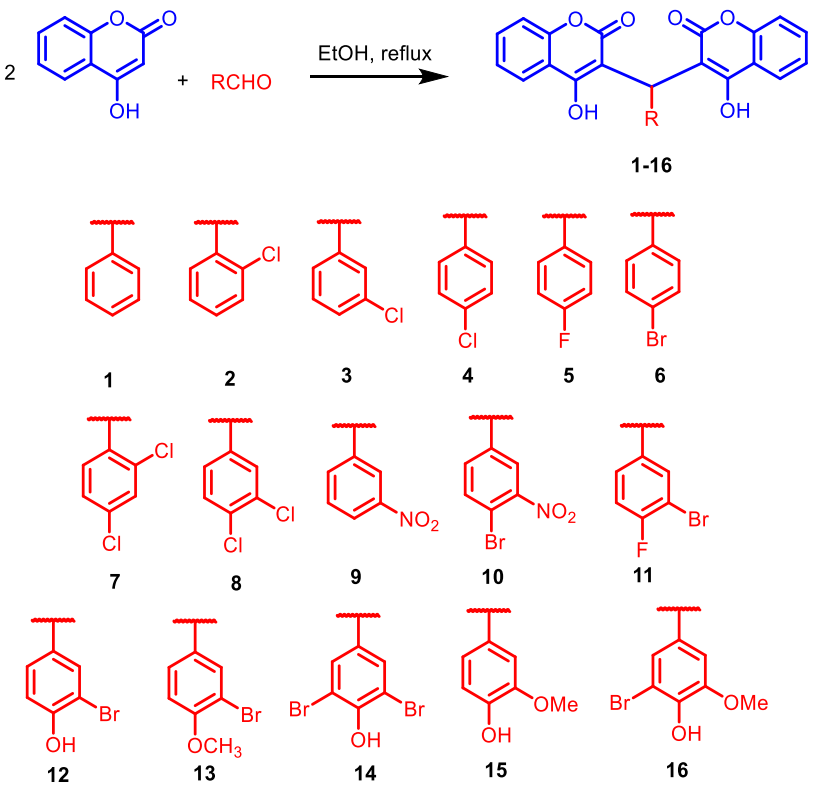

investigated on α-glucosidase inhibitors such as substituted coumarins,[23] hydroxycoumarin derivatives,[24] sulfonamide coumarins,[25] and biscoumarins (Figure 1).[26−29] However, there are a few reported synthetic biscoumarin derivatives that exhibit potent α-glucosidase inhibition. In addition, biscoumarins displayed a wide range of biological versatility.[30−41] This motivated us to design, synthesize biscoumarins, and evaluate biscoumarins for their inhibition effect and mechanism of action against α-glucosidase. In this research, we also performed quantitative structure−activity relationship (QSAR), molecular docking, molecular dynamics (MD) simulations, and fragment molecular orbital (FMO) method. The best active biscoumarin derivative could be further studied as a potential compound for the treatment of diabetes.

RESULTS AND DISCUSSION

Synthesis of Biscoumarins 1−16 and Their Inhibition against α-Glucosidase. To study QSAR of halogenated

https://doi.org/10.1021/acsomega.3c02868
ACS Omega 2023, 8, 26340−26350

biscoumarins, 16 derivatives **1**−**16** (Scheme 1) were synthesized and tested against α-glucosidase. The inhibitory activity of these compounds at a concentration of 10 μM was screened, and their IC_{50} values were subsequently evaluated. The results are shown in Figure 2 and Table 1. In general, the

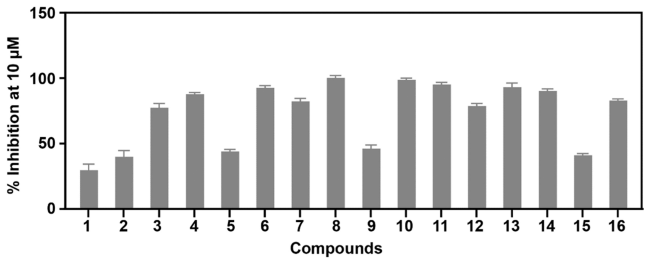

Figure 2. α-Glucosidase inhibition of biscoumarin derivatives **1**−**16**.

synthesized derivatives showed better activity compared to the positive control (acarbose, IC_{50} = 93.63 μM) and starting material (4-hydroxycoumarin, IC_{50} > 200 μM). In addition, the substituents on the phenyl ring of the benzaldehydes affected the inhibition of α-glucosidase. The inhibition of compounds **2**−**16** was much higher than that of the unsubstituted biscoumarin **1**.

Almost all biscoumarins containing halogen exhibited good to excellent inhibitory activity. Replacement of *m*-chloro with *m*-nitro led to reduced inhibitory activity, as observed in **3** and **9**. Moreover, the introduction of a chloro group at different positions resulted in different inhibitory activities (**2**−**4**, **7**, and **8**). The activity was enhanced by placing the chloro substituent at the *p*-position.

Additionally, among chloro, fluoro, and bromo (**4**−**6**), the F group obviously led to lower inhibitory activity. The best result was obtained with *p*-bromo in biscoumarin **6** with an IC_{50} of 2.95 μM. It was worth noting that adding the bromo group at the *m*-position in compound **11** improved the inhibition to 2.89 μM compared to **5** bearing fluoro at the *p*-position (IC_{50} 12.31 μM). The same effect could be seen when the inhibitory activities of **12** and **14**, **15** and **16**, or **9** and **10** (bromo at the *p*-position) were compared. When the bromo group was replaced by an electron-donating group like methoxy, the inhibitory activity decreased three times as in **12** and **15**. Taken together, the above findings suggest that the existence of bromo was the most favorable to enhance the inhibitory activity against α-glucosidase.

QSAR Study. The α-glucosidase inhibitory activity and physical and chemical properties of 16 biscoumarin derivatives were analyzed using the Materials Studio program (MS)[42] to establish a quantitative structure−activity relationship (QSAR) model. The model was developed using genetic algorithm (GA)-based multiple linear regression (MLR) techniques. The best obtained QSAR model as shown in eq 1 was used to predict the α-glucosidase inhibitory activity of biscoumarin derivatives with reasonable accuracy. The square correlation coefficient (R^2) value was 0.835. Additionally, the cross-validated square correlation coefficient (Q^2) with a value of 0.747 affirmed the robustness of this obtained model

$$pIC_{50} = 0.547 \times [\text{Alog P98}] + 0.024 \times [\text{shadow area: } XY \text{ plane}] - 1.923 \quad (1)$$

According to the intuitive observations of the model, the high lipophilicity of the biscoumarin series (AlogP98) had a great positive effect on the inhibition of α-glucosidase. Combining the above discussions of 16 compounds that introducing more halogen groups was pivotal to enhance the inhibitory activities, this speculation was consistent with the previous consensus in the field of drug discovery that halogen substituents will increase the lipophilicity of molecules,[43] which will help improve the penetration through the cell's lipid membrane, especially when the halogen element became bulky and more polarized functional groups, leading to a corresponding increase in the London dispersion forces. Moreover, expanding the shadow area of the *XY* plane, which corresponded to the *p*-substituent of the R group, could bring about a moderate increase in the α-glucosidase suppression performance of biscoumarin derivatives. Thus, the bulky substitutions could slightly support the inhibitory activity of α-glucosidase, as found in a comparison between compounds **12** and **13**.

According to Figure 3, the QSAR results suggested that biscoumarins bearing 3,5-dibromo and 4-alkoxy groups may be potent compounds to study α-glucosidase inhibition further. Inspired by the result and aiming to investigate potent inhibitors, we synthesized three new compounds **17**−**19** according to the procedure in Scheme 1. Their inhibitory activity against α-glucosidase was determined. Interestingly, as expected, biscoumarin **17** enhanced the activity slightly compared to monobromo biscoumarin **13**. **18** and **19** displayed excellent activity with IC_{50} values of 0.62 ± 0.01 and 1.21 ± 0.16 μM, respectively. The long-chain alkoxy substituent ($-OC_4H_9$, $-OC_8H_{17}$) at the *p*-position on the phenyl ring of benzaldehyde was highly preferred.

Kinetic Study and Binding of Halogenated Biscoumarins to α-Glucosidase. The enzyme kinetic study was performed to study the inhibition mode of **17**−**19** against α-glucosidase. The activity was determined at different concentrations of *p*-nitrophenyl-α-D-glucopyranoside (pNPG) in the presence or absence of **17**−**19** and analyzed using Lineweaver−Burk plots. As can be seen in Figure 4A, K_m increased, while V_{max} values were unaffected. Therefore, this study indicated that compounds **17**−**19** should be competitive inhibitors for α-glucosidase. The K_i values 4.81, 3.93, and 1.80 μM were calculated directly by the secondary replot of the

Table 1. *In Vitro* **α-Glucosidase Inhibitory Activities of Biscoumarins 1−16**

compound	IC_{50} (μM)	compound	IC_{50} (μM)	compound	IC_{50} (μM)
1	30.77 ± 1.25	**7**	3.15 ± 0.31	**13**	3.80 ± 0.05
2	8.12 ± 0.59	**8**	1.90 ± 0.14	**14**	2.38 ± 0.24
3	6.06 ± 0.06	**9**	14.80 ± 0.32	**15**	15.23 ± 0.45
4	3.19 ± 0.41	**10**	3.41 ± 0.17	**16**	5.10 ± 0.18
5	12.31 ± 0.08	**11**	2.89 ± 0.25	acarbose	93.63 ± 0.49
6	2.95 ± 0.05	**12**	4.15 ± 0.06		

https://doi.org/10.1021/acsomega.3c02868
ACS Omega 2023, 8, 26340−26350

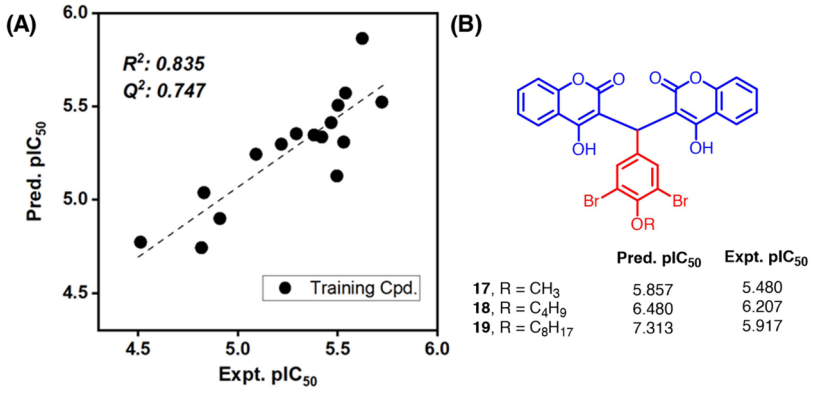

Figure 3. (A) Experimental pIC_{50} versus predicted pIC_{50} from the QSAR model (compounds **1**−**16**). (B) Compounds **17**, **18**, and **19** are newly designed candidate biscoumarin compounds.

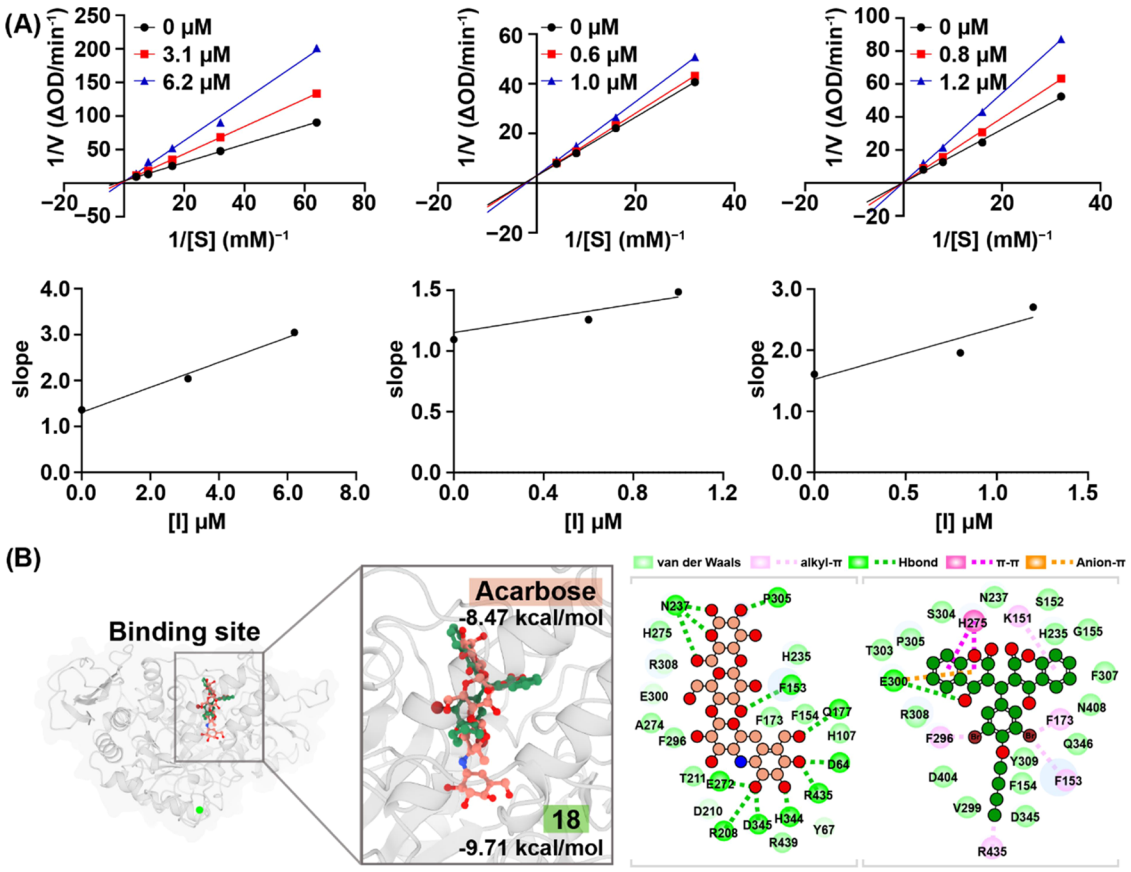

Figure 4. (A) Kinetic study of **17**−**19**. The Lineweaver−Burk plot for α-glucosidase inhibition and plots of slope versus concentration of **17**−**19** for determining the inhibition constant K_i. (B) Molecular docking analysis of acarbose (a native inhibitor) and **18** with α-glucosidase.

Lineweaver−Burk plots against the different concentrations of **17**, **18**, and **19**, respectively.

The binding affinity of acarbose and designed biscoumarins (**17**−**19**) was evaluated by docking them to the original binding site (OBS) of α-glucosidase MAL12. The docking results and inhibitory activity are presented in Table 2 and Figure 4B. **18** exhibited the most promising inhibitory potential by targeting the OBS of α-glucosidase MAL12 as a competitive inhibitor, based on the binding affinity score obtained from the molecular docking study. Computational studies provided insight into the molecular mechanism by which **18** inhibits the α-glucosidase activity. Compound **18** was found to be accessible to the OBS of the α-glucosidase, similar to acarbose, the native inhibitor, as shown in Figure 4B. The binding poses of these compounds were also similar, with

Table 2. Molecular Docking Results and Inhibitory Activity of Acarbose and 17−19 against α-Glucosidase

	binding affinity score (kcal/mol)	IC_{50} (μM)	%inhibition (10 μM)
17	−9.00	3.31 ± 0.03	99.77 ± 0.49
18	−9.71	0.62 ± 0.01	99.67 ± 0.42
19	−8.90	1.21 ± 0.16	98.95 ± 0.26
acarbose	−8.47	93.63 ± 0.49[a]	-[b]

[a]Data according to the literature. [b]-, not determined.

https://doi.org/10.1021/acsomega.3c02868
ACS Omega 2023, 8, 26340−26350

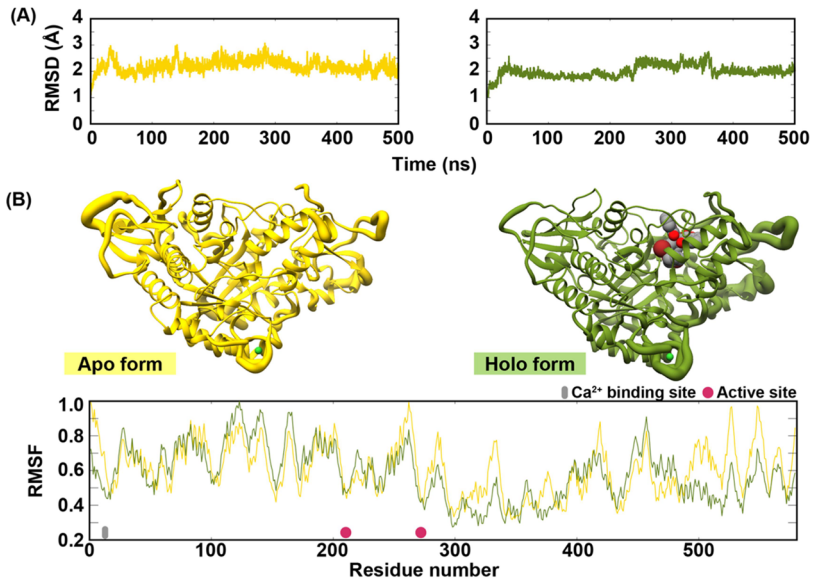

Figure 5. Structural analysis of α-glucosidase by comparing (A) Cα-RMSD and (B) the normalized RMSF between apo (yellow) and holo (green) forms.

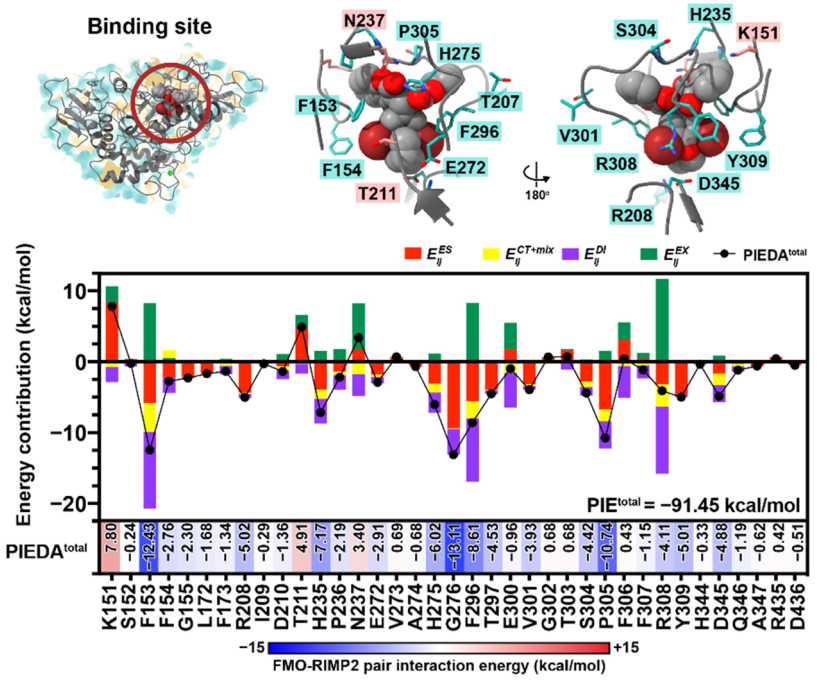

Figure 6. Analysis of the binding pattern and interaction profile between **18** and α-glucosidase at the OBS using the FMO-RIMP2 method. The electrostatic (red), charge-transfer (yellow), dispersion (purple), and charge exchange (green) interactions of key residues with **18** are depicted, with the amino acids having $PIEDA^{total}$ values <−3 or >3 kcal/mol labeled.

the isomaltotriose group of acarbose aligned with one 4-hydroxycoumarin ring in biscoumarin **18**. The residues N237, H275, E300, and P305 interacted with this moiety in both systems. Additionally, the core structure of acarbose and the 3,5-dibromo-4-butoxybenzene group of **18** revealed similar binding poses and common interacting residues, which were hydrophobic amino acids, such as F153, F154, F173, and F296. Although **18** did not show any interaction with the maltose-binding region, the double size of the 4-hydroxycoumarin ring could block the OBS entry pore by forming several hydrophobic interactions, such as $\pi-\pi$, alkyl$-\pi$, and anion$-\pi$, with nearby amino acids at the OBS.

Dynamics and Binding Efficiency of Potent Compound. The binding of biscoumarin **18** to α-glucosidase at the OBS was found to be stable during the 500 ns MD simulation, and the resulting structural dynamics were compared with the apo form of the enzyme in Figure 5. The root-mean-square deviation (RMSD) value showed that the overall system had a lower fluctuation in the bound complex (2.00 ± 0.20 Å) relative to the apo form (2.20 ± 0.25 Å), as shown in Figure 5A. The normalized root-mean-square fluctuation (RMSF) was calculated for the free enzyme and **18**-bound complex over the last 100 ns, revealing flexible and rigid domains in the protein (Figure 5B). Compared to the apo system, the residues 226–

https://doi.org/10.1021/acsomega.3c02868
ACS Omega 2023, 8, 26340−26350

230, 270−275, and 300−360 with lower RMSF values were relatively stable in the **18**-bound complex, indicating that the ligand restricts protein motion and binding site dynamics.[44] The binding free energy of the **18**/α-glucosidase complex of −21.74 ± 0.65 kcal/mol was estimated using the MM/GBSA method, showing a primary interaction toward α-glucosidase (−65.76 ± 0.32 kcal/mol) through van der Waals forces (Table S2 in the Supporting Information).

The presence of halogen atoms in a potent inhibitor prompted quantum mechanics calculations to investigate their influence on the binding interaction with the protein target.[45−47] The FMO-RIMP2 method was used to calculate the total pair interaction energy (PIEDA^{total}) between **18** and bound residues within 7 Å of the representative structure derived from RMSD clustering, revealing a robust binding interaction (−91.45 kcal/mol). The PIEDA was further decomposed into each interacting residue, as shown in Figure 6. The dispersion (E_{IJ}^{DI}) and charge-transfer (E_{IJ}^{CT+mix}) interactions between bromo substituents and nearby residues (F153, F154, F296, and Y309) were found to be crucial for enhancing the binding strength and stability to the OBS of α-glucosidase. Additionally, the electrostatic energy (E_{IJ}^{ES}) between bromine and Y309, combined with the hydrophobic interaction from H235, H275, G276, and S304 at the entry pore of the OBS, was also essential for **18** to maintain its binding in this site and reduce enzyme activity. Although the electrostatic interaction (E_{IJ}^{ES}), E_{IJ}^{DI}, and E_{IJ}^{CT+mix} in R308 displayed a good PIEDA value, it showed a moderate PIEDA^{total}, which could be attributed to the presence of steric hindrance to **18** considered by charge exchange (E_{IJ}^{EX}). Moreover, the repulsive effects caused by E_{IJ}^{ES} and E_{IJ}^{EX} found in K151, T211, and N237 might affect ligand mobility. Overall, these findings provide insight into the role of brominated biscoumarin in α-glucosidase inhibition and highlight the importance of specific interactions with key residues in enhancing the binding affinity and stability of the inhibitor.

CONCLUSIONS

In summary, biscoumarin derivatives, especially halogenated compounds, were successfully synthesized and their inhibitory activity toward α-glucosidase was evaluated. The result revealed that all synthesized derivatives exhibited prominent inhibitory activity with IC_{50} values of 0.62−30.77 μM. The enzyme kinetic study confirmed the competitive binding mode of the potential compound **18** with a K_i value of 3.93 μM. The computational study revealed that **18** could fit into the binding site of α-glucosidase MAL12 and create several hydrophobic interactions with the adjacent amino acids. The present findings suggest that biscoumarins containing 3,5-dibromo substituents and long-chain alkoxy groups at the *p*-position on the phenyl ring could be promising compounds for further study of α-glucosidase inhibitory activity.

EXPERIMENTAL SECTION

Chemistry. α-Glucosidase from *Saccharomyces cerevisiae* (EC 3.2.1.20) and pNPG were supplied by Sigma-Aldrich. All of the other commercially available reagents were used without further purification. ^{1}H and ^{13}C NMR spectra were recorded in $CDCl_3$ or DMSO-d_6 using a JEOL NMR 500 MHz spectrometer for ^{1}H and 125 MHz for ^{13}C. All solvents used in this research were distilled prior to use except those that were reagent grades. Thin-layer chromatography (TLC) was performed on aluminum sheets precoated with silica gel (Merck Kieselgel 60 PF254).

General Procedures. 4-Hydroxycoumarin (2 equiv) was dissolved in ethanol, and benzaldehyde (1 equiv) was added. The mixture was refluxed until a precipitate occurred within approximately 24 h. After that, the reaction was cooled down. The precipitates were filtered and washed with ethanol to obtain pure products **1**−**19**.

3,3′-(Phenylmethylene)bis(4-hydroxy-2H-chromen-2-one) ***1***. White solid; yield 70.3%; R_f (dichloromethane/methanol/acetic acid; 8:1:0.01) = 0.57; 100.00% purity by HPLC; ^{1}H NMR (500 MHz, $CDCl_3$) δ_H (ppm) 11.53 (s, 1H), 11.30 (s, 1H), 8.07 (d, J = 8.0 Hz, 1H), 8.00 (d, J = 7.5 Hz, 1H), 7.65−7.61 (m, 2H), 7.42−7.38 (m, 4H), 7.34−7.31 (m, 2H), 7.29−7.27 (m, 1H), 7.24−7.22 (m, 2H), and 6.11 (d, J = 1.0 Hz, 1H); ^{13}C NMR (125 MHz, $CDCl_3$) δ_C (ppm) 169.4, 167.0, 165.9, 164.7, 152.7, 152.4, 135.3, 133.0 (2C), 128.8 (2C), 127.0, 126.6 (2C), 125.0 (2C), 124.5 (2C), 117.0, 116.8 (2C), 116.6, 105.8, 104.0, and 36.3.

3,3′-((2-Chlorophenyl)methylene)bis(4-hydroxy-2H-chromen-2-one) ***2***. White solid; yield 72.0%; R_f (dichloromethane/methanol/acetic acid; 8:1:0.01) = 0.48; 99.27% purity by HPLC; ^{1}H NMR (500 MHz, $CDCl_3$) δ_H (ppm) 11.64 (s, 1H), 10.93 (s, 1H), 8.06 (s, 1H), 8.00 (s, 1H), 7.62 (m, 2H), 7.47−7.45 (m, 1H), 7.40−7.37 (m, 4H), 7.36−7.35 (m, 1H), 7.29−7.26 (m, 1H), 7.26−7.22 (m, 1H), 6.14 (s, 1H); ^{13}C NMR (125 MHz, $CDCl_3$) δ_C (ppm) 168.9, 167.3, 165.3, 164.4, 152.6, 152.2, 133.6, 133.6, 133.0 (2C), 130.9, 129.4, 128.7, 126.9, 125.0 (2C), 124.5 (2C), 116.9, 116.7 (2C), 116.5, 105.8, 104.5, and 35.8.

3,3′-((3-Chlorophenyl)methylene)bis(4-hydroxy-2H-chromen-2-one) ***3***. White solid; yield 75.0%; R_f (dichloromethane/methanol/acetic acid; 8:1:0.01) = 0.54; 99.94% purity by HPLC; ^{1}H NMR (500 MHz, $CDCl_3$) δ_H (ppm) 11.53 (s, 1H), 11.29 (s, 1H), 8.07 (d, J = 8.5 Hz, 1H), 8.01 (d, J = 8.0 Hz, 1H), 7.66−7.63 (m, 2H), 7.43−7.38 (m, 4H), 7.26 (m, 1H), 7.25 (d, 1H, J = 1.0 Hz), 7.19−7.18 (m, 1H), 7.13−7.10 (m, 1H), and 6.05 (s, 1H); ^{13}C NMR (125 MHz, $CDCl_3$) δ_C (ppm) 169.3, 167.0, 166.2, 164.8, 152.7, 152.4, 137.7, 134.8, 133.2 (2C), 130.0, 127.3, 126.8, 125.1 (2C), 124.9, 124.6 (2C), 116.9, 116.9, 116.8, 116.5, 105.3, 103.6, and 36.1.

3,3′-((4-Chlorophenyl)methylene)bis(4-hydroxy-2H-chromen-2-one) ***4***. White solid; yield 62.1%; R_f (dichloromethane/methanol/acetic acid; 8:1:0.01) = 0.54; 99.41% purity by HPLC; ^{1}H NMR (500 MHz, $CDCl_3$) δ_H (ppm) 11.54 (s, 1H), 11.32 (s, 1H), 8.06 (d, J = 8.0 Hz, 1H), 7.99 (d, J = 8.5 Hz, 1H), 7.65−7.62 (m, 2H), 7.42−7.38 (m, 4H), 7.30−7.29 (m, 1H), 7.28−7.27 (m, 1H), 7.16 (m, 1H), 7.14 (m, 1H), 6.04 (s, 1H); ^{13}C NMR (125 MHz, $CDCl_3$) δ_C (ppm) 169.3, 167.0, 166.1, 164.7, 152.6, 152.4, 134.0, 133.2 (2C), 132.8, 128.9 (2C), 128.1 (2C), 125.1 (2C), 124.5 (2C), 116.9, 116.8, 116.8, 116.4, 105.4, 103.8, and 35.9.

3,3′-((4-Fluorophenyl)methylene)bis(4-hydroxy-2H-chromen-2-one) ***5***. White solid; yield 65.7%; R_f (dichloromethane/methanol/acetic acid; 8:1:0.01) = 0.51; 98.54% purity by HPLC; ^{1}H NMR (500 MHz, $CDCl_3$) δ_H (ppm) 11.54 (s, 1H), 11.32 (s, 1H), 8.07 (1H, d, J = 7.0 Hz), 8.00 (d, J = 8.0 Hz, 1H), 7.65−7.62 (m, 2H), 7.42−7.37 (m, 4H), 7.20−7.17 (m, 2H), 7.03−6.99 (m, 2H), 6.05 (s, 1H); ^{13}C NMR (125 MHz, $CDCl_3$) δ_C (ppm) 169.4, 167.0, 166.0, 164.8, 161.8 (d, J = 244.1 Hz, 1C), 152.6, 152.4, 133.1 (2C), 130.9 (d, J = 3.5 Hz, 1C), 128.2 (d, J = 7.8 Hz, 2C), 125.1 (2C), 124.5 (2C), 117.0,

https://doi.org/10.1021/acsomega.3c02868
ACS Omega 2023, 8, 26340−26350

116.8 (2C), 116.5, 115.6 (d, J = 21.4 Hz, 2C), 105.6, 104.0, and 35.8.

3,3′-((4-Bromophenyl)methylene)bis(4-hydroxy-2H-chromen-2-one) ***6***. White solid; yield 65.0%; R_f (dichloromethane/methanol/acetic acid; 8:1:0.01) = 0.51; 99.16% purity by HPLC; ^{1}H NMR (500 MHz, $CDCl_3$) δ_H (ppm) 11.54 (s, 1H), 11.32 (s, 1H), 8.06 (d, J = 8.0 Hz, 1H), 7.99 (d, J = 8.0 Hz, 1H), 7.64 (m, 2H), 7.44−7.41 (m, 4H), 7.41−7.40 (m, 2H), 7.11−7.09 (m, 2H), and 6.01 (t, J = 1.5 Hz, 1H); ^{13}C NMR (125 MHz, $CDCl_3$) δ_C (ppm) 169.4, 167.0, 166.2, 164.8, 152.6, 152.4, 134.5, 133.2 (2C), 131.8 (2C), 128.5 (2C), 125.1 (2C), 124.5 (2C), 120.9, 116.9, 116.8, 116.8, 116.4, 105.3, 103.7, and 36.0.

3,3′-((2,4-Dichlorophenyl)methylene)bis(4-hydroxy-2H-chromen-2-one) ***7***. White solid; yield 65.5%; R_f (dichloromethane/methanol/acetic acid; 8:1:0.01) = 0.46; 99.27% purity by HPLC; ^{1}H NMR (500 MHz, $CDCl_3$) δ_H (ppm) 11.67 (s, 1H), 10.93 (s, 1H), 8.04 (s, 1H), 8.00 (s, 1H), 7.64−7.61 (m, 2H), 7.40−7.39 (m, 4H), 7.37−7.36 (m, 2H), 7.24 (dd, J = 8.5, 2.5 Hz, 1H), and 6.08 (d, J = 1.0 Hz, 1H); ^{13}C NMR (125 MHz, $CDCl_3$) δ_C (ppm) 168.8, 167.4, 165.5, 164.7, 152.5, 152.3, 134.3, 133.8, 133.2 (2C), 132.4, 130.7, 130.3, 127.1, 125.1 (2C), 124.6 (2C), 116.8 (2C), 116.4 (2C), 105.4, 104.2, and 35.5.

3,3′-((3,4-Dichlorophenyl)methylene)bis(4-hydroxy-2H-chromen-2-one) ***8***. White solid; yield 8.2%; R_f (dichloromethane/methanol/acetic acid; 8:1:0.01) = 0.48; 99.20% purity by HPLC; ^{1}H NMR (500 MHz, DMSO-d_6) δ_H (ppm) 7.87 (dd, J = 8.0, 1.5 Hz, 2H), 7.58−7.55 (m, 2H), 7.45 (d, J = 8.0 Hz, 1H), 7.32 (d, J = 7.5 Hz, 2H), 7.30−7.27 (m, 3H), 7.14−7.11 (m, 1H), 6.27 (s, 1H); ^{13}C NMR (125 MHz, DMSO-d_6) δ_C (ppm) 166.5 (2C), 164.5 (2C), 152.5 (2C), 142.9, 131.8 (2C), 130.6, 130.1, 128.7, 127.9, 127.5, 124.1 (2C), 123.5 (2C), 118.7 (2C), 115.9 (2C), 103.3 (2C), and 35.9.

3,3′-((3-Nitrophenyl)methylene)bis(4-hydroxy-2H-chromen-2-one) ***9***. White solid; yield 55.4%; R_f (dichloromethane/methanol/acetic acid; 8:1:0.01) = 0.46; 96.11% purity by HPLC; ^{1}H NMR (500 MHz, $CDCl_3$) δ_H (ppm) 11.58 (s, 1H), 11.38 (s, 1H), 8.17−8.13 (m, 1H), 8.08 (d, J = 8.0 Hz, 1H), 8.06 (m, 1H), 7.99 (d, J = 8.0 Hz, 1H), 7.69−7.65 (m, 2H), 7.59−7.56 (m, 1H), 7.51 (t, J = 8.0 Hz, 1H), 7.44 (m, 2H), 7.43−7.38 (m, 2H), 6.12 (d, J = 1.5 Hz, 1H); ^{13}C NMR (125 MHz, $CDCl_3$) δ_C (ppm) 169.2, 167.1, 166.7, 165.0, 152.7, 152.4, 148.8, 138.1, 133.5 (2C), 132.9, 129.7, 125.3, 125.3, 124.6, 124.6, 122.2, 121.9, 116.9, 116.8, 116.8, 116.4, 104.7, 103.3, and 36.3.

3,3′-((4-Bromo-3-nitrophenyl)methylene)bis(4-hydroxy-2H-chromen-2-one) ***10***. White solid; yield 22.3%; R_f (dichloromethane/methanol/acetic acid; 8:1:0.01) = 0.43; 99.51% purity by HPLC; ^{1}H NMR (500 MHz, $CDCl_3$) δ_H (ppm) 11.58 (s, 1H), 11.37 (s, 1H), 8.08 (d, J = 8.0 Hz, 1H), 7.99 (d, J = 8.0 Hz, 1H), 7.69−7.68 (m, 2H), 7.67−7.65 (m, 2H), 7.44−7.40 (m, 4H), 7.31−7.29 (m, 1H), 6.03 (t, J = 1.5 Hz, 1H); ^{13}C NMR (125 MHz, $CDCl_3$) δ_C (ppm) 169.2, 167.0, 166.9, 165.0, 152.7, 152.5, 150.1, 137.4, 136.4, 133.6 (2C), 131.7, 125.4, 124.7 (2C), 124.2 (2C), 117.0, 116.9, 116.7, 116.3, 113.0, 104.3, 103.0, and 36.0; HRMS (ESI) calcd for $C_{25}H_{14}BrNO_8$ $[M + H]^+$: 535.9981, found 535.9982.

3,3′-((3-Bromo-4-fluorophenyl)methylene)bis(4-hydroxy-2H-chromen-2-one) ***11***. White solid; yield 42.8%; R_f (dichloromethane/methanol/acetic acid; 8:1:0.01) = 0.48; 99.38% purity by HPLC; ^{1}H NMR (500 MHz, $CDCl_3$) δ_H (ppm) 11.57 (s, 1H), 11.30 (s, 1H), 8.07 (d, J = 7.5 Hz, 1H), 8.00 (d, J = 8.0 Hz, 1H), 7.65 (m, 2H), 7.43−7.39 (m, 4H), 7.38−7.36 (m, 1H), 7.16−7.12 (m, 1H), 7.07 (t, J = 8.5 Hz, 1H), and 6.03 (t, J = 1.5 Hz, 1H); ^{13}C NMR (125 MHz, $CDCl_3$) δ_C (ppm) 169.2, 167.3, 166.3, 164.9, 158.0 (d, J = 245.6 Hz, 1C), 152.7, 152.4, 133.3 (2C), 132.9 (d, J = 3.6 Hz, 1C), 131.7, 127.3 (d, J = 7.0 Hz, 1C), 125.2 (2C), 124.6 (2C), 116.9, 116.8, 116.6 (d, J = 22.2 Hz, 1C), 116.4 (2C), 109.5 (d, J = 21.4 Hz, 1C), 105.1, 103.6, and 35.6.

3,3′-((3-Bromo-4-hydroxyphenyl)methylene)bis(4-hydroxy-2H-chromen-2-one) ***12***. White solid; yield 38.9%; R_f (dichloromethane/methanol/acetic acid; 8:1:0.01) = 0.34; 98.75% purity by HPLC; ^{1}H NMR (500 MHz, $CDCl_3$) δ_H (ppm) 11.55 (s, 1H), 11.28 (s, 1H), 8.06 (d, J = 8.0 Hz, 1H), 8.00 (d, J = 7.5 Hz, 1H), 7.64 (m, 2H), 7.42−7.37 (m, 4H), 7.27 (m, 1H), 7.08−7.06 (m, 1H), 6.96 (d, J = 8.5 Hz, 1H), and 6.01 (t, J = 1.5 Hz, 1H); ^{13}C NMR (125 MHz, $CDCl_3$) δ_C (ppm) 169.3, 166.9, 166.1, 164.8, 152.7, 152.4, 151.3, 133.2 (2C), 130.1, 129.0, 127.6, 125.1 (2C), 124.6 (2C), 116.8, 116.8 (2C), 116.3 (2C), 110.7, 105.4, 103.8, and 35.4; HRMS (ESI) calcd for $C_{25}H_{15}BrO_7$ $[M + H]^+$: 507.0079, found 507.0074.

3,3′-((3-Bromo-4-methoxyphenyl)methylene)bis(4-hydroxy-2H-chromen-2-one) ***13***. White solid; yield 82.1%; R_f (dichloromethane/methanol/acetic acid; 8:1:0.01) = 0.57; 98.89% purity by HPLC; ^{1}H NMR (500 MHz, $CDCl_3$) δ_H (ppm) 11.55 (s, 1H), 11.28 (s, 1H), 8.06 (d, J = 8.0 Hz, 1H), 8.00 (d, J = 8.0 Hz, 1H), 7.64 (m, 2H), 7.42−7.38 (m, 4H), 7.35 (m, 1H), 7.11 (m, 1H), 6.84 (d, J = 7.5 Hz, 1H), 6.02 (t, J = 1.5 Hz, 1H), and 3.88 (s, 3H); ^{13}C NMR (125 MHz, $CDCl_3$) δ_C (ppm) 169.3, 166.9, 166.1, 164.8, 154.9, 152.7, 152.4, 133.1 (2C), 131.4, 128.9, 126.8, 125.1 (2C), 124.6 (2C), 117.0, 116.8 (2C), 116.5, 112.1, 111.9, 105.4, 103.9, 56.4, and 35.3.

3,3′-((3,5-Dibromo-4-hydroxyphenyl)methylene)bis(4-hydroxy-2H-chromen-2-one) ***14***. White solid; yield 68.3%; R_f (dichloromethane/methanol/acetic acid; 8:1:0.01) = 0.43; 99.36% purity by HPLC; ^{1}H NMR (500 MHz, DMSO-d_6) δ_H (ppm) 7.87 (dd, J = 8.0, 2.0 Hz, 2H), 7.56 (m, 2H), 7.32 (dd, J = 8.0, 1.0 Hz, 2H), 7.29 (m, 2H), 7.20 (d, J = 1.0 Hz, 2H), and 6.20 (t, J = 1.0 Hz, 1H); ^{13}C NMR (125 MHz, DMSO-d_6) δ_C (ppm) 166.5 (2C), 164.4 (2C), 152.4 (2C), 148.4, 135.9, 131.7 (2C), 130.4 (2C), 124.1 (2C), 123.5 (2C), 118.7 (2C), 115.9 (2C), 111.8 (2C), 103.3 (2C), and 35.2.

3,3′-((4-Hydroxy-3-methoxyphenyl)methylene)bis(4-hydroxy-2H-chromen-2-one) ***15***. White solid; yield 80.2%; R_f (dichloromethane/methanol/acetic acid; 8:1:0.01) = 0.37; 99.26% purity by HPLC; ^{1}H NMR (500 MHz, $CDCl_3$) δ_H (ppm) 11.52 (s, 1H), 11.28 (s, 1H), 8.06 (brs, 1H), 8.02 (brs, 1H), 7.63 (m, 2H), 7.41−7.40 (m, 4H), 6.86 (d, J = 8.0 Hz, 1H), 6.73−6.71 (m, 1H), 6.68 (m, 1H), 6.06 (t, J = 1.0 Hz, 1H), and 3.75 (s, 3H); ^{13}C NMR (125 MHz, $CDCl_3$) δ_C (ppm) 169.4, 166.9, 165.8, 164.8, 152.6 (2C), 146.8, 144.7, 133.0, 127.0 (2C), 125.0 (2C), 124.5 (2C), 119.6, 116.8 (4C), 114.6, 109.6, 105.9, 104.3, 56.2, and 35.9.

3,3′-((3-Bromo-4-hydroxy-5-methoxyphenyl)methylene)-bis(4-hydroxy-2H-chromen-2-one) ***16***. White solid; yield 83.4%; R_f (dichloromethane/methanol/acetic acid; 8:1:0.01) = 0.40; 99.85% purity by HPLC; ^{1}H NMR (500 MHz, $CDCl_3$) δ_H (ppm) 11.56 (s, 1H), 11.26 (s, 1H), 8.06 (d, J = 7.5 Hz, 1H), 8.01 (d, J = 8.0 Hz, 1H), 7.64 (m, 2H), 7.42−7.40 (m, 4H), 6.92 (t, J = 1.5 Hz, 1H), 6.64 (d, J = 1.0 Hz, 1H), 6.03 (t, J = 1.0 Hz, 1H), and 3.76 (s, 3H); ^{13}C NMR (125 MHz,

https://doi.org/10.1021/acsomega.3c02868
ACS Omega 2023, 8, 26340−26350

$CDCl_3$) δ_C (ppm) 169.4, 166.8, 166.1, 164.8, 152.4 (2C), 147.4, 142.2, 133.2, 128.1 (2C), 125.1, 124.5 (2C), 122.8 (2C), 116.8 (4C), 109.0, 108.6, 105.4, 103.8, 56.6, 35.7; DART-MS calcd for $C_{26}H_{17}BrO_8$ $[M + H]^+$: 537.0185, found 537.0244.

To a solution of 3,5-dibromo-4-hydroxybenzaldehyde (0.84 g, 3 mmol), methyl iodide or alkyl bromides (6.6 mmol) and anhydrous potassium carbonate (K_2CO_3, 0.828 g, 6 mmol) in DMF (10 mL) were added. The reaction mixture was stirred at 55 °C for 3 h, cooled to room temperature, and quenched with the addition of water (80 mL). The resulting white precipitate was filtered under vacuum, washed with water (40 mL), and dried to give the anisaldehyde intermediate (0.72 g, 2.44 mmol, 81.4%) as a white solid, R_f (*n*-hexane/ethyl acetate; 30:1) = 0.51.[48] For the reaction with 1-bromobutane or 1-bromooctane, after the reaction was completed (analyzed by TLC), the crude product was extracted with EtOAc (3 × 20 mL), and the combined extracts were washed with water. The organic layer was dried over anhydrous Na_2SO_4 and evaporated to dryness. The synthesized 3,5-dibromo-4-alkoxybenzaldehydes yielded as a light yellow oil (50.0% yield); R_f (*n*-hexane/ethyl acetate; 30:1) = 0.51 was used to synthesize biscoumarins without further purification.

3,3′-((3,5-Dibromo-4-methoxyphenyl)methylene)bis(4-hydroxy-2H-chromen-2-one) ***17.*** White solid; yield 21.0%; R_f (CH_2Cl_2/MeOH/AcOH; 8:1:0.01) = 0.51; 96.63% purity by HPLC; ^{1}H NMR (500 MHz, $CDCl_3$) δ_H (ppm) 11.60 (s, 1H), 11.28 (s, 1H), 8.07 (d, J = 8.0 Hz, 1H), 8.02 (d, J = 8.0 Hz, 1H), 7.66 (m, 2H), 7.43−7.40 (m, 4H), 7.31 (d, J = 1.0 Hz, 2H), 6.00 (t, J = 1.0 Hz, 1H), and 3.89 (s, 3H); ^{13}C NMR (125 MHz, $CDCl_3$) δ_C (ppm) 169.2, 166.9, 166.4, 164.9, 153.1, 152.7, 152.4, 134.4, 133.4 (2C), 130.9 (2C), 125.2 (2C), 124.6 (2C), 118.5 (2C), 117.0 (2C), 116.8 (2C), 104.8, 103.3, 60.8, and 35.4; HRMS (ESI) calcd for $C_{26}H_{16}Br_2O_7$ $[M + H]^+$: 598.9341, found 598.9283.

3,3′-((3,5-Dibromo-4-butoxyphenyl)methylene)bis(4-hydroxy-2H-chromen-2-one) ***18.*** White solid; yield 54.0%; R_f (CH_2Cl_2/MeOH/AcOH; 8:1:0.01) = 0.54; 98.53% purity by HPLC; ^{1}H NMR (500 MHz, $CDCl_3$) δ_H (ppm) 11.59 (s,1H), 11.27 (s, 1H), 8.06 (d, J = 7.5 Hz, 1H), 8.02 (d, J = 8.0 Hz, 1H), 7.65 (td, J = 7.5, 1.5 Hz, 2H), 7.43−7.40 (m, 4H), 7.31 (d, J = 1.5 Hz, 2H), 6.00 (t, J = 1.0 Hz, 1H), 4.01 (t, J = 6.5 Hz, 2H), 1.84 (quint, J = 6.5 Hz, 2H), 1.59−1.54 (m, 2H), and 1.00 (t, J = 7.5 Hz, 3H); ^{13}C NMR (125 MHz, $CDCl_3$) δ_C (ppm) 169.2, 166.9, 166.4, 164.9, 152.7, 152.5, 152.4, 134.0, 133.4 (2C), 130.8 (2C), 125.2 (2C), 124.6 (2C), 118.8 (2C), 116.9, 116.8 (2C), 116.4, 104.8, 103.3, 73.5, 35.4, 32.2, 19.3, and 14.1; HRMS (ESI) calcd for $C_{29}H_{22}Br_2O_7$ $[M + H]^+$: 640.9811, found 640.9805.

3,3′-((3,5-Dibromo-4-(octyloxy)phenyl)methylene)bis(4-hydroxy-2H-chromen-2-one) ***19.*** White solid; yield 50.6%; R_f (CH_2Cl_2/MeOH/AcOH; 8:1:0.01) = 0.63; 99.46% purity by HPLC; ^{1}H NMR (500 MHz, $CDCl_3$) δ_H (ppm) 11.59 (s, 1H), 11.27 (s, 1H), 8.07 (d, J = 8.0 Hz, 1H), 8.02 (d, J = 8.0 Hz, 1H), 7.65 (td, J = 7.5, 1.5 Hz, 2H), 7.43−7.38 (m, 4H), 7.30 (d, J = 1.5 Hz, 2H), 6.00 (t, J = 1.0 Hz, 1H), 4.00 (t, J = 6.5 Hz, 2H), 1.86 (quint, J = 6.5 Hz, 2H), 1.52 (quint, J = 6.5 Hz, 2H), 1.38−1.29 (m, 8H), and 0.88 (t, J = 6.5 Hz, 3H); ^{13}C NMR (125 MHz, $CDCl_3$) δ_C (ppm) 169.2, 166.9, 166.4, 164.9, 152.7, 152.5, 152.4, 134.0, 133.4 (2C), 130.8 (2C), 125.2 (2C), 124.6 (2C), 118.8 (2C), 116.9, 116.8 (2C), 116.4, 104.8, 103.3, 73.8, 35.4, 32.0, 30.2, 29.5, 29.4, 26.0, 22.8, and 14.2; DART-MS (ESI) calcd for $C_{33}H_{30}Br_2O_7$ $[M + H]^+$: 697.0437, found 697.0509.

Inhibition of α-Glucosidase Activity *In Vitro*. The α-glucosidase inhibition of the synthesized compounds **1−19** was measured using a spectrophotometric method.[49] Those compounds (4 mM) were dissolved in DMSO and diluted by 0.1 mM pH 6.9 phosphate buffer. The enzyme α-glucosidase from *S. cerevisiae* E.C. 3.2.1.20 (0.1 U/mL) and 1 mM pNPG as the substrate were dissolved in 0.1 mM pH 6.9 phosphate buffer. Then, 10 μL of a test compound or a positive control was added with 40 μL of the enzyme, and the mixture was then incubated at 37 °C for 10 min. Afterward, 50 μL of the substrate was added to the reaction mixture. The mixture was incubated further for 20 min at 37 °C, and then 1 M of Na_2CO_3 (100 μL) was added to stop the reaction. The activity was measured at 405 nm (Allsheng microplate reader, AMR100). All samples were analyzed in triplicate at different concentrations to obtain the IC_{50} values of each compound. The mean values and standard deviation were calculated. The percentage inhibition was calculated by the following equation

$$\%\text{inhibition} = \left(1 - \frac{A_{\text{sample}}}{A_{\text{control}}}\right) \times 100 \quad (2)$$

where % inhibition is the percentage of inhibition, A_{sample} is the corrected absorbance of the synthesized compound under test $[A_{\text{sample(initial)}} - A_{\text{blank-sample}}]$, and A_{control} is the absorbance of the negative control.

QSAR Modeling. The three-dimensional (3D) structures of all biscoumarin derivatives were imported into the QSAR module of Material Studio (MS) software.[42] In addition, 16 structural descriptors (**1−16**) generated via the model module in MS were selected as the independent variables. All molecular descriptors could be grouped into several categories: structural descriptors, thermodynamic descriptors, topological descriptors, E-state keys, fragment counts, shadow indices, spatial descriptors, and VAMP electrostatic descriptors. In addition, the α-glucosidase inhibitory experimental values in the unit of IC_{50} (μM) were transformed to be pIC_{50} (M) values, which act as the response data.

The statistics module in the MS program was used to establish the QSAR model to predict the inhibitory activity of α-glucosidase. First, the descriptor selection was performed via the genetic algorithm methods provided by the genetic function approximation[50] (GFA) of the MS package. The 3000 population size, 200 maximum generations, and Friedman's lack-of-fitness function[51] were used for the GFA process. The regressions were carried out using two-five descriptors, and R^2 and Q^2 were monitored.

Molecular Docking, MD Simulation, and FMO Calculation. The 3D structure of α-glucosidase MAL12 was obtained from the alphafold2 database[52,53] due to the lack of crystal structure available in the protein database. The 3D structure of acarbose, **17**, **18**, and **19** was constructed using GaussView 6.0.16 and optimized by Gaussian16 using the HF/6-31G+(d,p) basis set.[54] Since the designed biscoumarins consist of halogen atoms, the complex structure was prepared by molecular docking using the AutoDock VinaXB program,[55−57] which contains the halogen force field parameters. Acarbose and designed biscoumarins were docked to the original receptor binding site (OBS) with the grid dimensions of 16 × 16 × 16 Å^3.[58] The binding pattern of these compounds and their interaction were carried out using two-dimensional

https://doi.org/10.1021/acsomega.3c02868
ACS Omega 2023, 8, 26340−26350

(2D) and 3D using Discovery Studio Visualizer Software[59] and Chimera USCF.[60] The MD trajectory was analyzed with regrading to the structural stability by RMSF and RMSD techniques using the Cpptraj module implemented in the AmberTools 21.[61] The last 100 ns trajectories were used to calculate the binding free energy between **18** and α-glucosidase using the MM/GBSA method.[62]

The fragment molecular orbital method using the second-order Møller−Plesset perturbation theory with the resolution-of-identity approximation (FMO-RIMP2) at the B3LYP3/6-31G+(d,p) level of theory was applied for the representative model of **18**/α-glucosidase complex extracted from the last 100 ns trajectories using RMSD clustering techniques.[63,64] The pair interaction energy (PIE) can be additionally decayed into four terms of interaction: electrostatic (E_{IJ}^{ES}), exchange (E_{IJ}^{EX}), charge-transfer (E_{IJ}^{CT+mix}), and dispersion (E_{IJ}^{DI}) contributions, which are called PIEDA (eq 3).[65] These contributed energies can explain the essential halogen-containing compounds[66]

$$E_{IJ}^{PIE} = E_{IJ}^{ES} + E_{IJ}^{EX} + E_{IJ}^{CT+mix} + E_{IJ}^{DI} \quad (3)$$

■ ASSOCIATED CONTENT

Supporting Information

The Supporting Information is available free of charge at https://pubs.acs.org/doi/10.1021/acsomega.3c02868.

^{1}H and ^{13}C NMR spectra, HPLC analysis of synthesized compounds **1**−**19**, HRMS of **10**, **12**, **17**, **18**, DART-MS of **16** and **19** (Figures S1−S63), SMILES (Table S1), and MM/GBSA binding free energy ($\Delta G_{bind}^{MM/GBSA}$) for **18** binding to α-glucosidase at the OBS site (Table S2) (PDF)

■ AUTHOR INFORMATION

Corresponding Author

Warinthorn Chavasiri − *Center of Excellence in Natural Products Chemistry, Department of Chemistry, Faculty of Science, Chulalongkorn University, Bangkok 10330, Thailand;* orcid.org/0000-0001-5201-1324; Email: warinthorn.c@chula.ac.th

Authors

Thi-Hong-Truc Phan − *Center of Excellence in Natural Products Chemistry, Department of Chemistry, Faculty of Science, Chulalongkorn University, Bangkok 10330, Thailand*

Kowit Hengphasatporn − *Center for Computational Sciences, University of Tsukuba, Tsukuba, Ibaraki 305-8577, Japan;* orcid.org/0000-0001-8501-3844

Yasuteru Shigeta − *Center for Computational Sciences, University of Tsukuba, Tsukuba, Ibaraki 305-8577, Japan;* orcid.org/0000-0002-3219-6007

Wanting Xie − *Research Center of Nano Science and Technology, Shanghai University, Shanghai 200444, People's Republic of China*

Phornphimon Maitarad − *Research Center of Nano Science and Technology, Shanghai University, Shanghai 200444, People's Republic of China;* orcid.org/0000-0003-0035-0070

Thanyada Rungrotmongkol − *Program in Bioinformatics and Computational Biology, Graduated School, Chulalongkorn University, Bangkok 10330, Thailand; Center of Excellence in Structural and Computational Biology, Department of Biochemistry, Faculty of Science, Chulalongkorn University, Bangkok 10330, Thailand;* orcid.org/0000-0002-7402-3235

Complete contact information is available at: https://pubs.acs.org/10.1021/acsomega.3c02868

Notes

The authors declare no competing financial interest.

■ ACKNOWLEDGMENTS

This work was financially supported by the ASEAN Scholarship.

■ ABBREVIATIONS

OBS, original binding site; HCV, hepatitis C virus; HIV, human immunodeficiency virus; QSAR, quantitative structure−activity relationship; MS, Material Studio program; GA, genetic algorithm; MLR, multiple linear regression; MD, molecular dynamics; RMSF, root-mean-square fluctuation; RMSD, root-mean-square deviation; pNPG, *p*-nitrophenyl-α-D-glucopyranoside

■ REFERENCES

(1) Ghani, U. Re-exploring promising α-glucosidase inhibitors for potential development into oral anti-diabetic drugs: Finding needle in the haystack. *Eur. J. Med. Chem.* **2015**, *103*, 133−162.

(2) Pan, Y.; Liu, T.; Wang, X.; Sun, J. Research progress of coumarins and their derivatives in the treatment of diabetes. *J. Enzyme Inhib. Med. Chem.* **2022**, *37*, 616−628.

(3) Dove, A. Seeking sweet relief for diabetes. *Nat. Biotechnol.* **2002**, *20*, 977−981.

(4) Tan, M.-H. α-Glucosidase inhibitors in the treatment of diabetes. *Curr. Opin. Endocrinol. Diabetes Obes.* **1997**, *4*, 48−55.

(5) Laar, F. Alpha-glucosidase inhibitors in the early treatment of type 2 diabetes. *Vasc. Health Risk. Manag.* **2008**, *4*, 1189−1195.

(6) Jacob, G. S. Glycosylation inhibitors in biology and medicine. *Curr. Opin. Struct. Biol.* **1995**, *5*, 605−611.

(7) Zhang, L.; Chen, Q.; Li, L.; Kwong, J. S.; Jia, P.; Zhao, P.; Wang, W.; Zhou, X.; Zhang, M.; Sun, X. Alpha-glucosidase inhibitors and hepatotoxicity in type 2 diabetes: a systematic review and meta-analysis. *Sci. Rep.* **2016**, *6*, No. 32649.

(8) Krentz, A. J.; Bailey, C. J. Oral antidiabetic agents. *Drugs* **2005**, *65*, 385−411.

(9) Ueberschaar, N.; Xu, Z.; Scherlach, K.; Metsä-Ketelä, M.; Bretschneider, T.; Dahse, H.-M.; Görls, H.; Hertweck, C. Synthetic remodeling of the chartreusin pathway to tune antiproliferative and antibacterial activities. *J. Am. Chem. Soc.* **2013**, *135*, 17408−17416.

(10) Amin, K. M.; Abou-Seri, S. M.; Awadallah, F. M.; Eissa, A. A.; Hassan, G. S.; Abdulla, M. M. Synthesis and anticancer activity of some 8-substituted-7-methoxy-2H-chromen-2-one derivatives toward hepatocellular carcinoma HepG2 cells. *Eur. J. Med. Chem.* **2015**, *90*, 221−231.

(11) Liu, M.-M.; Chen, X.-Y.; Huang, Y.-Q.; Feng, P.; Guo, Y.-L.; Yang, G.; Chen, Y. Hybrids of phenylsulfonylfuroxan and coumarin as potent antitumor agents. *J. Med. Chem.* **2014**, *57*, 9343−9356.

(12) Tsay, S.-C.; Hwu, J. R.; Singha, R.; Huang, W.-C.; Chang, Y. H.; Hsu, M.-H.; Shieh, F.-k.; Lin, C.-C.; Hwang, K. C.; Horng, J.-C.; et al. Coumarins hinged directly on benzimidazoles and their ribofuranosides to inhibit hepatitis C virus. *Eur. J. Med. Chem.* **2013**, *63*, 290−298.

(13) Kamiyama, H.; Kubo, Y.; Sato, H.; Yamamoto, N.; Fukuda, T.; Ishibashi, F.; Iwao, M. Synthesis, structure−activity relationships, and mechanism of action of anti-HIV-1 lamellarin α-20-sulfate analogues. *Bioorg. Med. Chem.* **2011**, *19*, 7541−7550.

(14) Shaik, J. B.; Palaka, B. K.; Penumala, M.; Kotapati, K. V.; Devineni, S. R.; Eadlapalli, S.; Darla, M. M.; Ampasala, D. R.; Vadde, R.; Amooru, G. D. Synthesis, pharmacological assessment, molecular modeling and in silico studies of fused tricyclic coumarin derivatives as a new family of multifunctional anti-Alzheimer agents. *Eur. J. Med. Chem.* **2016**, *107*, 219−232.
(15) Sashidhara, K. V.; Kumar, A.; Dodda, R. P.; Krishna, N. N.; Agarwal, P.; Srivastava, K.; Puri, S. Coumarin−trioxane hybrids: Synthesis and evaluation as a new class of antimalarial scaffolds. *Bioorg. Med. Chem. Lett.* **2012**, *22*, 3926−3930.
(16) Pingaew, R.; Saekee, A.; Mandi, P.; Nantasenamat, C.; Prachayasittikul, S.; Ruchirawat, S.; Prachayasittikul, V. Synthesis, biological evaluation and molecular docking of novel chalcone-coumarin hybrids as anticancer and antimalarial agents. *Eur. J. Med. Chem.* **2014**, *85*, 65−76.
(17) Hu, Y.-Q.; Xu, Z.; Zhang, S.; Wu, X.; Ding, J.-W.; Lv, Z.-S.; Feng, L.-S. Recent developments of coumarin-containing derivatives and their anti-tubercular activity. *Eur. J. Med. Chem.* **2017**, *136*, 122−130.
(18) Puttaraju, K. B.; Shivashankar, K.; Mahendra, M.; Rasal, V. P.; Vivek, P. N. V.; Rai, K.; Chanu, M. B. Microwave assisted synthesis of dihydrobenzo[4,5]imidazo[1,2-α] pyrimidin-4-ones; synthesis, in vitro antimicrobial and anticancer activities of novel coumarin substituted dihydrobenzo[4,5]imidazo [1,2-α]pyrimidin-4-ones. *Eur. J. Med. Chem.* **2013**, *69*, 316−322.
(19) Nagamallu, R.; Srinivasan, B.; Ningappa, M. B.; Kariyappa, A. K. Synthesis of novel coumarin appended bis(formylpyrazole) derivatives: Studies on their antimicrobial and antioxidant activities. *Bioorg. Med. Chem. Lett.* **2016**, *26*, 690−694.
(20) Amin, K. M.; Rahman, D. E. A.; Al-Eryani, Y. A. Synthesis and preliminary evaluation of some substituted coumarins as anticonvulsant agents. *Bioorg. Med. Chem. Lett.* **2008**, *16*, 5377−5388.
(21) Aggarwal, R.; Kumar, S.; Kaushik, P.; Kaushik, D.; Gupta, G. K. Synthesis and pharmacological evaluation of some novel 2-(5-hydroxy-5-trifluoromethyl-4,5-dihydropyrazol-1-yl)4-(coumarin-3-yl)-thiazoles. *Eur. J. Med. Chem.* **2013**, *62*, 508−514.
(22) Ibrar, A.; Shehzadi, S. A.; Saeed, F.; Khan, I. Developing hybrid molecule therapeutics for diverse enzyme inhibitory action: Active role of coumarin-based structural leads in drug discovery. *Bioorg. Med. Chem.* **2018**, *26*, 3731−3762.
(23) Raju, B. C.; Tiwari, A. K.; Kumar, J. A.; Ali, A. Z.; Agawane, S. B.; Saidachary, G.; Madhusudana, K. α-Glucosidase inhibitory antihyperglycemic activity of substituted chromenone derivatives. *Bioorg. Med. Chem.* **2010**, *18*, 358−365.
(24) Shen, Q.; Shao, J.; Peng, Q.; Zhang, W.; Ma, L.; Chan, A. S.; Gu, L. Hydroxycoumarin derivatives: Novel and potent α-glucosidase inhibitors. *J. Med. Chem.* **2010**, *53*, 8252−8259.
(25) Wang, S.; Yan, J.; Wang, X.; Yang, Z.; Lin, F.; Zhang, T. Synthesis and evaluation of the α-glucosidase inhibitory activity of 3-[4-(phenylsulfonamido)benzoyl]-2*H*-1-benzopyran-2-one derivatives. *Eur. J. Med. Chem.* **2010**, *45*, 1250−1255.
(26) Khan, K. M.; Rahim, F.; Wadood, A.; Kosar, N.; Taha, M.; Lalani, S.; Khan, A.; Fakhri, M. I.; Junaid, M.; Rehman, W.; et al. Synthesis and molecular docking studies of potent α-glucosidase inhibitors based on biscoumarin skeleton. *Eur. J. Med. Chem.* **2014**, *81*, 245−252.
(27) Zawawi, N. K. N. A.; Taha, M.; Ahmat, N.; Ismail, N. H.; Wadood, A.; Rahim, F.; Rehman, A. U. Synthesis, in vitro evaluation and molecular docking studies of biscoumarin thiourea as a new inhibitor of α-glucosidases. *Bioorg. Chem.* **2015**, *63*, 36−44.
(28) Asgari, M. S.; Mohammadi-Khanaposhtani, M.; Kiani, M.; Ranjbar, P. R.; Zabihi, E.; Pourbagher, R.; Rahimi, R.; Faramarzi, M. A.; Biglar, M.; Larijani, B.; et al. Biscoumarin-1, 2, 3-triazole hybrids as novel anti-diabetic agents: Design, synthesis, in vitro α-glucosidase inhibition, kinetic, and docking studies. *Bioorg. Chem.* **2019**, *92*, No. 103206.
(29) Mohammadi-Khanaposhtani, M.; Yahyavi, H.; Barzegaric, E.; Imanparast, S.; Faramarzi, M. A.; et al. New biscoumarin derivatives as potent α-glucosidase inhibitors: Synthesis, biological evaluation, kinetic analysis, and docking study. *Polycyclic Aromat. Compd.* **2020**, *40*, 915−926.
(30) Zhao, H.; Neamati, N.; Hong, H.; Mazumder, A.; Wang, S.; Sunder, S.; Milne, G. W.; Pommier, Y.; Burke, T. R. Coumarin-based inhibitors of HIV integrase. *J. Med. Chem.* **1997**, *40*, 242−249.
(31) Khan, K. M.; Iqbal, S.; Lodhi, M. A.; Maharvi, G. M.; Choudhary, M. I.; Perveen, S.; et al. Biscoumarin: new class of urease inhibitors; economical synthesis and activity. *Bioorg. Med. Chem.* **2004**, *12*, 1963−1968.
(32) Lodhi, M. A.; Nawaz, S. A.; Iqbal, S.; Khan, K. M.; Rode, B. M.; Choudhary, M. I.; et al. 3D-QSAR CoMFA studies on bis-coumarine analogues as urease inhibitors: A strategic design in anti-urease agents. *Bioorg. Med. Chem.* **2008**, *16*, 3456−3461.
(33) Arif Lodhi, M.; Wadood, A.; Iqbal, S.; Khan, K. M.; Choudhary, M. I.; et al. Three-dimensional quantitative structure−activity relationship (CoMSIA) analysis of bis-coumerine analogues as urease inhibitors. *Med. Chem. Res.* **2013**, *22*, 498−504.
(34) Lodhi, M. A.; Shams, S.; Choudhary, M. I.; Lodhi, A.; Ul-Haq, Z.; Jalil, S.; Nawaz, S. A.; Khan, K. M.; Iqbal, S.; Rahman, A.-u. Structural basis of binding and rationale for the potent urease inhibitory activity of biscoumarins. *Biomed Res. Int.* **2014**, *2014*, No. 935039.
(35) Faisal, M.; Saeed, A.; Shahzad, D.; Fattah, T. A.; Lal, B.; Channar, P. A.; Mahar, J.; Saeed, S.; Mahesar, P. A.; Larik, F. A. Enzyme inhibitory activities an insight into the structure−Activity relationship of biscoumarin derivatives. *Eur. J. Med. Chem.* **2017**, *141*, 386−403.
(36) Alomari, M.; Taha, M.; Imran, S.; Jamil, W.; Selvaraj, M.; Uddin, N.; Rahim, F. Design, synthesis, in vitro evaluation, molecular docking and ADME properties studies of hybrid bis-coumarin with thiadiazole as a new inhibitor of Urease. *Bioorg. Chem.* **2019**, *92*, No. 103235.
(37) Salar, U.; Nizamani, A.; Arshad, F.; Khan, K. M.; Fakhri, M. I.; Perveen, S.; Ahmed, N.; Choudhary, M. I. Bis-coumarins; non-cytotoxic selective urease inhibitors and antiglycation agents. *Bioorg. Chem.* **2019**, *91*, No. 103170.
(38) Mukhtar, F.; Stieglitz, K.; Ali, S.; Ejaz, A.; Choudhary, M. I.; Fakhri, M. I.; Salar, U.; Khan, K. M. Coumarin and biscoumarin inhibit *in vitro* obesity model. *Adv. Biol. Chem.* **2016**, *6*, No. 71593.
(39) Rahim, F.; Ullah, H.; Fakhri, M. I.; Salar, U.; Perveen, S.; Khan, K. M.; Choudhary, M. I. Anti-Leishmanial Activities of Synthetic Biscoumarins. *J. Chem. Soc. Pak.* **2017**, *39*, 79−82.
(40) Mayank; Kumar, D.; Kaur, N.; Giri, R.; Singh, N. A biscoumarin scaffold as an efficient anti-Zika virus lead with NS3-helicase inhibitory potential: in vitro and in silico investigations. *New J. Chem.* **2020**, *44*, 1872−1880.
(41) Ullah, H.; Fahad, K. Synthetic Biscoumarin Analogs: Their PC3 Cell Line and Antioxidant Inhibitory Potentials. *J. Ongoing Chem. Res.* **2020**, *5*, 1−6.
(42) *Materials Studio Modeling;release 7.0*; Accelrys Software Inc., 2013.
(43) Wilcken, R.; Zimmermann, M. O.; Lange, A.; Joerger, A. C.; Boeckler, F. M. Principles and applications of halogen bonding in medicinal chemistry and chemical biology. *J. Med. Chem.* **2013**, *56*, 1363−1388.
(44) Sakulkeo, O.; Wattanapiromsakul, C.; Pitakbut, T.; Dej-adisai, S. Alpha-glucosidase inhibition and molecular docking of isolated compounds from traditional Thai medicinal plant, *Neuropeltis racemosa* Wall. *Molecules* **2022**, *27*, 639.
(45) Lin, F.-Y.; MacKerell, A. D., Jr Do halogen−hydrogen bond donor interactions dominate the favorable contribution of halogens to ligand−protein binding? *J. Phys. Chem. B* **2017**, *121*, 6813−6821.
(46) Marzec, E.; Świtalska, M.; Winiewska-Szajewska, M.; Wójcik, J.; Wietrzyk, J.; Maciejewska, A. M.; Poznański, J.; Mieczkowski, A. The halogenation of natural flavonoids, baicalein and chrysin, enhances their affinity to human protein kinase CK2. *IUBMB Life* **2020**, *72*, 1250−1261.
(47) Deetanya, P.; Hengphasatporn, K.; Wilasluck, P.; Shigeta, Y.; Rungrotmongkol, T.; Wangkanont, K. Interaction of 8-anilinonaph-

https://doi.org/10.1021/acsomega.3c02868
ACS Omega 2023, 8, 26340−26350

thalene-1-sulfonate with SARS-CoV-2 main protease and its application as a fluorescent probe for inhibitor identification. *Comput. Struct. Biotechnol. J.* **2021**, *19*, 3364−3371.
(48) Takahashi, M.; Yamamoto, A.; Inuzuka, T.; Sengoku, T.; Yoda, H. Synthesis of lipophilic bisanthracene fluorophores: versatile building blocks toward the synthesis of new light-harvesting dendrimers. *Tetrahedron* **2011**, *67*, 9484−9490.
(49) Ramadhan, R.; Phuwapraisirisan, P. New arylalkanones from Horsfieldia macrobotrys, effective antidiabetic agents concomitantly inhibiting α-glucosidase and free radicals. *Bioorg. Med. Chem. Lett.* **2015**, *25*, 4529−4533.
(50) Wu, W.; Zhang, C.; Lin, W.; Chen, Q.; Guo, X.; Qian, Y.; Zhang, L. Quantitative structure-property relationship (QSPR) modeling of drug-loaded polymeric micelles via genetic function approximation. *PLoS One* **2015**, *10*, No. e0119575.
(51) Friedman, J. H. Multivariate adaptive regression splines. *Ann. Stat.* **1991**, *19*, 1−67.
(52) Jumper, J.; Evans, R.; Pritzel, A.; Green, T.; Figurnov, M.; Ronneberger, O.; Tunyasuvunakool, K.; Bates, R.; Žídek, A.; Potapenko, A.; et al. Highly accurate protein structure prediction with AlphaFold. *Nature* **2021**, *596*, 583−589.
(53) Varadi, M.; Anyango, S.; Deshpande, M.; Nair, S.; Natassia, C.; Yordanova, G.; Yuan, D.; Stroe, O.; Wood, G.; Laydon, A.; et al. AlphaFold Protein Structure Database: massively expanding the structural coverage of protein-sequence space with high-accuracy models. *Nucleic Acids Res.* **2022**, *50*, D439−D444.
(54) Frisch, M.; Trucks, G.; Schlegel, H.; Scuseria, G.; Robb, M.; Cheeseman, J.; Scalmani, G.; Barone, V.; Petersson, G.; Nakatsuji, H. *Gaussian 16*; Gaussian, Inc.: Wallingford, CT, 2016.
(55) Koebel, M. R.; Schmadeke, G.; Posner, R. G.; Sirimulla, S. AutoDock VinaXB: implementation of XBSF, new empirical halogen bond scoring function, into AutoDock Vina. *J. Cheminf.* **2016**, *8*, No. 27.
(56) Hengphasatporn, K.; Kaewmalai, B.; Jansongsaeng, S.; Badavath, V. N.; Saelee, T.; Chokmahasarn, T.; Khotavivattana, T.; Shigeta, Y.; Rungrotmongkol, T.; Boonyasuppayakorn, S. Alkyne-tagged apigenin, a chemical tool to navigate potential targets of flavonoid anti-dengue leads. *Molecules* **2021**, *26*, 6967.
(57) Hengphasatporn, K.; Wilasluck, P.; Deetanya, P.; Wangkanont, K.; Chavasiri, W.; Visitchanakun, P.; Leelahavanichkul, A.; Paunrat, W.; Boonyasuppayakorn, S.; Rungrotmongkol, T.; et al. Halogenated baicalein as a promising antiviral agent toward SARS-CoV-2 main protease. *J. Chem. Inf. Model.* **2022**, *62*, 1498−1509.
(58) Zafar, M.; Khan, H.; Rauf, A.; Khan, A.; Lodhi, M. A. In silico study of alkaloids as α-glucosidase inhibitors: Hope for the discovery of effective lead compounds. *Front. Endocrinol.* **2016**, *7*, No. 153.
(59) BIOVIA. *Dassault Systèmes, Discovery Studio Visualizer*; Dassault Systèmes: San Diego, 2021.
(60) Pettersen, E. F.; Goddard, T. D.; Huang, C. C.; Couch, G. S.; Greenblatt, D. M.; Meng, E. C.; Ferrin, T. E. UCSF Chimera—a visualization system for exploratory research and analysis. *J. Comput. Chem.* **2004**, *25*, 1605−1612.
(61) Case, D. A.; Belfon, K.; Ben-Shalom, I. Y.; Brozell, S. R.; Cerutti, D. S.; Cheatham, T. E., III; Cruzeiro, V. W. D.; Darden, T. A.; Duke, R. E.; Giambasu, G.; Gilson, M. K.; Gohlke, H.; Goetz, A. W.; Harris, R.; Izadi, S.; Izmailov, S. A.; Kasavajhala, K.; Kovalenko, A.; Krasny, R.; Kurtzman, T.; Lee, T. S.; LeGrand, S.; Li, P.; Lin, C.; Liu, J.; Luchko, T.; Luo, R.; Man, V.; Merz, K. M.; Miao, Y.; Mikhailovskii, O.; Monard, G.; Nguyen, H.; Onufriev, A.; Pan, F.; Pantano, S.; Qi, R.; Roe, D. R.; Roitberg, A.; Sagui, C.; Schott-Verdugo, S.; Shen, J.; Simmerling, C. L.; Skrynnikov, N. R.; Smith, J.; Swails, J.; Walker, R. C.; Wang, J.; Wilson, L.; Wolf, R. M.; Wu, X.; Xiong, Y.; Xue, Y.; York, D. M.; Kollman, P. A. *AMBER 2020*; University of California: San Francisco, 2020.
(62) Mishra, S. K.; Koča, J. Assessing the performance of MM/PBSA, MM/GBSA, and QM−MM/GBSA approaches on protein/carbohydrate complexes: effect of implicit solvent models, QM methods, and entropic contributions. *J. Phys. Chem. B* **2018**, *122*, 8113−8121.
(63) Pham, B. Q.; Gordon, M. S. Development of the FMO/RI-MP2 fully analytic gradient using a hybrid-distributed/shared memory programming model. *J. Chem. Theory Comput.* **2020**, *16*, 1039−1054.
(64) Nutho, B.; Mahalapbutr, P.; Hengphasatporn, K.; Pattaranggoon, N. C.; Simanon, N.; Shigeta, Y.; Hannongbua, S.; Rungrotmongkol, T. Why are lopinavir and ritonavir effective against the newly emerged coronavirus 2019? Atomistic insights into the inhibitory mechanisms. *Biochemistry* **2020**, *59*, 1769−1779.
(65) Fedorov, D. G.; Kitaura, K. Pair interaction energy decomposition analysis. *J. Comput. Chem.* **2007**, *28*, 222−237.
(66) Hengphasatporn, K.; Garon, A.; Wolschann, P.; Langer, T.; Yasuteru, S.; Huynh, T. N.; Chavasiri, W.; Saelee, T.; Boonyasuppayakorn, S.; Rungrotmongkol, T. Multiple virtual screening strategies for the discovery of novel compounds active against dengue virus: A hit identification study. *Sci. Pharm.* **2020**, *88*, No. 2.

https://doi.org/10.1021/acsomega.3c02868
ACS Omega 2023, 8, 26340−26350